A review of frictional sliding on brine-penetrated faults in salt

André Niemeijer[1], Martijn van den Ende[2], Chris Marone[3,4], Derek Elsworth[4], Chris Spiers[1]*

[1]Department of Earth Sciences, Utrecht University, The Netherlands; [2]Université Côte d'Azur, OCA, UMR Lagrange, France; [3]Dipartimento di Scienze della Terra La Sapienza Università di Roma, Italy, [4] Department of Geosciences, Pennsylvania State University, USA

** a.r.niemeijer@uu.nl*

ABSTRACT: We review and discuss experimental observations of the frictional sliding of porous, fluid saturated faults in salt. In previous work, granular salt has been used almost exclusively as an analogue for quartz under hydrothermal conditions due to its high solubility at room temperature. However, the frictional behavior of salt itself is of interest, since localized frictional or frictional-viscous shear might occur at low effective stresses, such as those expected if migrating brine permeates localized zones during salt tectonics or after cavern abandonment. Results from slide-hold-slide experiments, performed at room temperature and an effective normal stress of 1, 2.5 and 5 MPa, show that porous/granular faults in salt regain strength within hours. Slip-dependent weakening, velocity-weakening and stick-slip behavior were observed during sliding at constant velocity, implying significant potential for unstable, localized deformation under fluid-saturated conditions. The results demonstrate that localized frictional or frictional-viscous shear of salt could occur in fluid-permeated zones at interfaces between lithologies, is potentially unstable and might provide pathways for fluid expulsion.

1 Introduction

In studies of fault and earthquake mechanics, the transition from brittle to viscous behaviour with increasing depth, i.e. pressure and temperature, is an important topic, because earthquakes are unlikely to nucleate in viscously deforming faults. Fluid-assisted diffusion creep or pressure solution is an important mechanism operating in natural faults at upper- to mid-crustal conditions However, it is challenging to investigate the effects of pressure solution or other viscous mechanisms in natural fault rocks at laboratory time scale. In contrast, pressure solution processes are rapid in salt, even at room temperature, provided that the grain size is small enough. Fine-grained salt has therefore often been used as a rock analogue material to investigate the effects of viscous mechanisms such as pressure solution on fault strength and stability (e.g. Shimamoto 1986; Bos et al. 2000; Niemeijer & Spiers 2006).

In nature, salt is generally considered to be an efficient seal against fluid migration due to its ductile nature under typical stress and strain rate conditions. However, cases of brittle faulting and subsequent fluid infiltration in salt have been reported (Davison 2009; Schléder et al. 2008; Zhuo et al. 2013). Schléder et al (2008) performed detailed microstructural observations of veins in folded rock salt samples retrieved from an exploratory borehole. On the basis of the presence of euhedral to subhedral halite grains, indicating they grew in an open space and the presence of fluid inclusion bands, they concluded that the crack was generated by hydrofracturing of the rock salt due to the development of near lithostatic fluid pressure. Davison (2009) presents several observations of brittle faulting in salt from both outcrops and seismic data and concluded that fracturing and faulting in salt likely only occurs in the presence of high pore fluid pressure. Finally, Zhuo et al. (2013) used the similarity of biomarkers in oil and gas below and above halite beds to conclude that the halite beds in this example did not act as an efficient seal and that hydrocarbons migrated through brittle faults in the halite beds.

Since brittle faulting creates porosity and permeability, understanding the parameters that affect the frictional strength could be important. Here, we present a summary and review of experimental studies of frictional sliding of simulated salt gouges.

2 Experimental approaches

The fault friction experiments reported in this contribution have all been performed on simulated fault gouges sandwiched between different types of forcing blocks. In a seminal study in 1986, Shimamoto reported results from experiments cylindrical specimens of Tennessee sandstone with a pre-cut surface at a 30 º angle to the central axis, covered with a thin (0.3 mm) layer of fine-grained salt (Figure 1). In these types of experiments, the cylindrical sample assembly is jacketed in a low strength jacket and subjected to variable confining pressures up to several 100s of MPa within an oil- or gas-filled pressure vessel. Shear on the simulated fault is achieved by advancing a piston at a prescribed rate, shortening the assembly. During shortening, the fault area reduces, and confining pressure will need to be adjusted to maintain constant normal stress. Total displacement on the simulated fault is limited to a few mm by the potential rupture of the jacket. Another type of friction test is the double-direct shear set-up inside a biaxial loading frame (Figure 1b). In this set-up, two identical layers of typically fine-grained material (i.e. simulated gouge) are sandwiched by two square stainless steel side blocks (typically 5x5 cm) and one rectangular central block of the same width (typically 5x10 cm). Normal stress is applied using a servo-controlled horizontal ram and shear on the layers is achieved by advancing the central piston at a prescribed rate. The fault area remains constant during shear, but the gouge layer becomes thinner with increasing displacement as gouge material is pushed down out of the fault area. The final type of friction experiments reported here are rotary or ring shear experiments, in which the sample assembly can be ring or cylinder ring shaped (Figure 1c). In the case of experiments using a cylindrical set-up, rocks such as gabbro are typically used as “wall rock” and the gouge layer is confined by an outer Teflon ring.

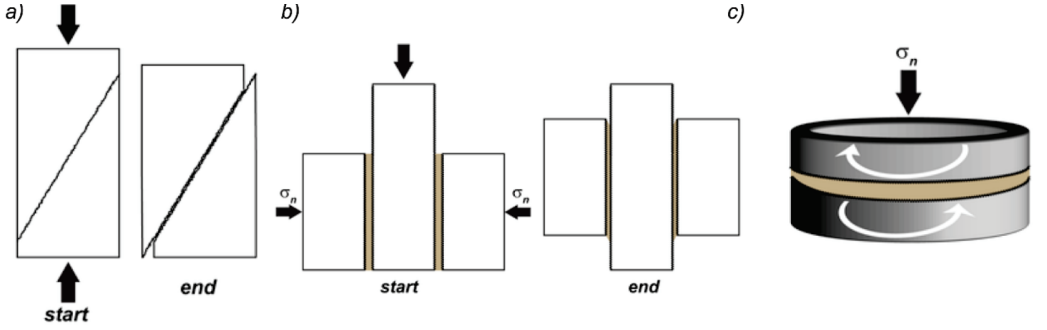

Figure 1: Diagrams of the different configurations used in the experiments reported here to investigate the frictional behaviour of simulated fault gouges. a) Saw-cut set-up, the gouge layer is sandwiched between two half cylinders cut typically at an angle of 25º to the vertical axis. b) Double-direct shear set-up, two gouge layers are sandwiched between roughened blocks, typically made of stainless-steel c) Ring shear set-up, a gouge layer is between two ring-shaped pistons (from Niemeijer et al. 2020).

In the experiments using a ring set-up, stainless rings are used, equipped with O-rings to provide a seal for pore fluids and confined by inner and outer stainless-steel rings. Importantly, in all types of experiments, the forcing blocks (“wall rocks”) are artificially roughened to promote slip to occur within the gouge layer. In the case of stainless steel or other metallic forcing blocks, machined regular triangular prisms (“teeth”) typically form the roughness. These teeth are regularly spaced and usually have a height of several 100s of

microns. In contrast, forcing blocks made from rocks are roughened by grinding with a sanding paper of specific roughness or by sandblasting. In all experiments, the procedure is to construct a simulated gouge layer by depositing and flattening a prescribed amount of granular salt with a known grain size distribution or fraction. The sample assembly consisting of the forcing blocks with the sandwiched gouge layer is subsequently installed in the deformation apparatus and a constant normal force is applied. In general, the sample is kept under a constant normal stress until changes in the layer thickness (compaction) are too small to measure. At this point, the secondary loading axis is engaged, and the sample is loaded in shear until slip occurs within the gouge layer. In most friction studies, the main interest is in the velocity dependence of sliding friction, expressed as an empirical variable *(a–b)*, which plays a key role in studies of earthquake nucleation using the empirical rate-and-state friction laws (RSF) (Dieterich 1979; Ruina 1983). The value of *(a–b)* is obtained by instantaneously changing the loading velocity and monitoring the change in friction:

$$(a-b) = \frac{\mu_1 - \mu_0}{\ln(v_1/v_0)}$$

where μ_0 is the steady state friction at v_0 and μ_1 is the steady state friction at v_1. In the RSF framework, a slip instability can only occur when *(a–b)* is negative and stable sliding occurs for positive values of *(a–b)*. A common goal of friction studies is thus to measure the variation in the value of *(a–b)* by shearing a sample at constant velocity until a steady state is reached followed by instantaneous changes in the loading velocity, typically at 3-fold increments (e.g. 1-3-10-30-100 μm/s). Often these types of velocity-step sequences are complemented by another procedure, so-called slide-hold-slides. In these, the loading velocity is set to zero for increasingly longer hold times and the peak friction upon re-sliding is determined and plotted as a function of hold time. In this way, a *healing* rate is determined as the loglinear slope through the data, which can be used to empirically extrapolate to natural temporal scales.

3 A note on extrapolation

In nature, seismic slip velocities are typically quoted to be in the order of m/s (Heaton 1990), whereas earthquake nucleation velocities are usually assumed to be on the order of μm/s (Marone 1998). However, it is not exactly known how to translate these to human-induced loading rates that are the consequence of changes in stress state due to the extraction or injection of fluids. A different type of experiment in which the shear stress on the simulated fault is controlled by injecting a fluid would closer mimic these cases (e.g. Scuderi & Collettini 2018). However, we can translate the loading rates shown in Figure 2 to the rates at which shear stress is applied using the stiffness of the experimental apparatuses. The lowest applicable laboratory rate of 0.001 μm/s translates to a stress change of ~0.1 kPa/s or 8.64 MPa per day, which is very high and makes a direct (empirical) extrapolation of laboratory results unreliable. It is therefore critical to identify the rate-controlling deformation mechanisms and use their kinetics to extrapolate laboratory results to nature.

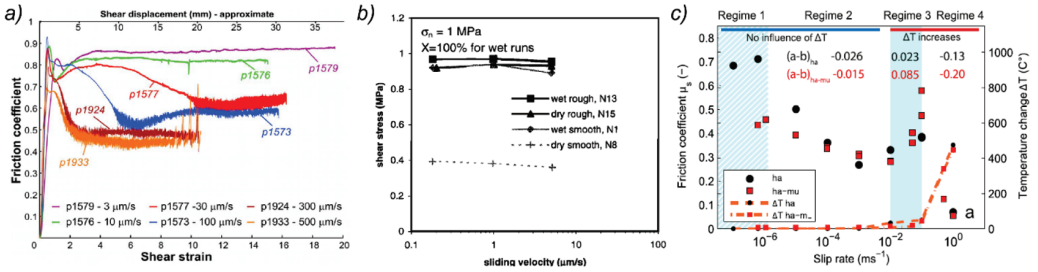

Figure 2: Results from frictional sliding experiments on simulated fault gouges of salt. a) Series of experiments at constant sliding in the presence of saturated brine at 5 MPa effective normal stress and with an initial layer thickness of 5 mm in the double direct shear set-up with steel forcing blocks (from Niemeijer et al 2010) b) Summary of velocity-stepping experiments in a rotary shear set-up with smooth and rough halite (< 3% porosity) wall rocks at 1 MPa effective normal stress in the presence of brine and with an initial layer thickness of 1 mm (from Bos et al. 2000). c) Summary of constant velocity-stepping experiments on 1 mm thick simulated fault gouges of salt (ha) and salt + 20 wt% gouge (ha-mu) at an effective normal stress of 5 MPa in a rotary shear apparatus with gabbro forcing blocks under room-dry conditions (from Buijze et al. 2017).

4 Velocity dependence of sliding strength of granular salt

In Figure 2, we show results from room temperature frictional sliding experiments on wet and room-dry granular salt gouges over a wide range of loading velocities. The steady state sliding strength depends strongly on the presence of a (chemically active) fluid, sliding velocity, displacement and the roughness of the wall rocks. At the lowest sliding velocities investigated (0.01- 10 µm/s), both room-dry and wet salt gouges have high frictional strength, with values between 0.7 to almost 1. Samples deformed dry are slightly weaker, but the difference is small compared to the effect of wall rock roughness and to that of higher slip velocities. Major weakening down to a friction of ~0.4 occurs for dry salt gouges deformed against a smooth wall rock (Figure 2b). A similar amount of weakening is observed for wet gouges deformed one to two orders of magnitude faster (v = 30-500 µm/s, Figure 2a) and even more weakening occurs in dry gouges sheared at 1 mm/s (Figure 2c). A similar observation of a broad velocity weakening was already made in 1986 by Shimamoto in saw-cut experiments on dry salt gouge performed at confining pressures up to 250 MPa. In those high confining pressure experiments, the transition from velocity strengthening to weakening occurred already at a velocity of 0.3 micron/s, which seems to decrease with increasing confining pressure. Note that the layer thickness in these experiments was only 0.3 mm.

It was noted by Shimamoto that some displacement is needed before a steady state mechanical behaviour is reached. This is also the case for wet salt gouges as shown in Figure 2a and was also demonstrated in the studies by Bos et al. (2000) and Buijze et al. (2017). The amount of displacement (or shear strain) needed to reach steady state sliding shortens with increasing sliding velocity and decreasing wall rock roughness (Niemeijer et al. 2010).

5 Failure or peak frictional strength of granular salt

Another interesting feature of the frictional strength of wet granular salt can be seen in Figure 2a. It seems that there can be quite a variability in the peak frictional strength of the gouge layers, which could be related to the loading velocity, but is more likely related to the duration of the pre-shear compaction stage. More detailed observations on this feature were made by Bos & Spiers (2002); Niemeijer et al (2008); van den Ende & Niemeijer (2019), by performing slide-hold-slide experiments on simulated fault gouges of brine-saturated salt. Some of their key results are shown in Figure 3. All three studies demonstrate that the failure strength of the simulated fault increases rapidly with increasing hold duration, particularly in brine-saturated samples. Moreover, the strength recovery is larger when the loading velocity is higher. The volumetric data shown in the bottom panel of Figure 3c indicate that there is a correlation between the strength recovery and the amount of compaction during the hold period. It seems that a higher porosity is sustained during sliding at higher velocity which allows for faster and more compaction during the hold periods, which in turn leads to a higher failure strength upon re-shear.

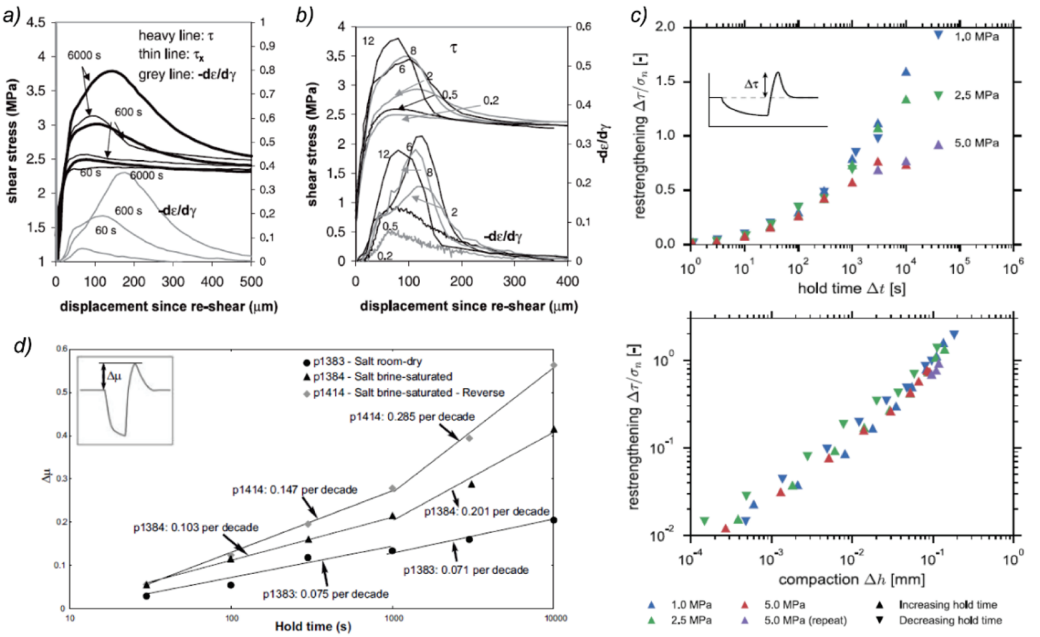

Figure 3. Experimental results of slide-hold-slide experiments on brine-saturated and room-dry salt gouges a), b) Experiments in a rotary shear set-up an effective normal stress of 2.5 MPa (from Bos & Spiers 2002). Sliding velocity was 2 μm/s in the experiments shown in a) with variable hold times, hold time was 600 seconds with variable loading velocities in b). c) Results from the same rotary shear set-up as Bos & Spiers (2002) with a loading velocity of 10 μm/s (from Van den Ende & Niemeijer 2019). Data shows the amount of excess frictional strength developed during the holds relative to the steady state sliding friction. Bottom panel shows the same data but plotted as a function of observed compaction during the hold. d) Results from the double-direct shear configuration at a loading rate of 5 μm/s and an effective normal stress of 5 MPa (from Niemeijer et al. 2008).

The data in the bottom panel of Figure 3c shows a loglinear relation between the strength recovery and the amount of compaction during the hold but this seems to deviate at larger values of compaction. In Figure 4 we can see why this is the case. In the shear stress vs.

normal stress plots for different hold periods, it becomes clear that the intercept at zero normal stress is no longer negligible for hold periods longer than 300 seconds. The slopes (=internal friction) and intercepts (=cohesion) are shown in Figures 4b and 4c, respectively. The strength recovery observed is not only due to the recovery of porosity lost during the hold period, but also due to the development of cohesion, which is likely to be the results of some form of grain boundary (contact) healing. Importantly, this suggests that the reactivation of brittle faults will require substantial shear stress even at zero effective normal stress.

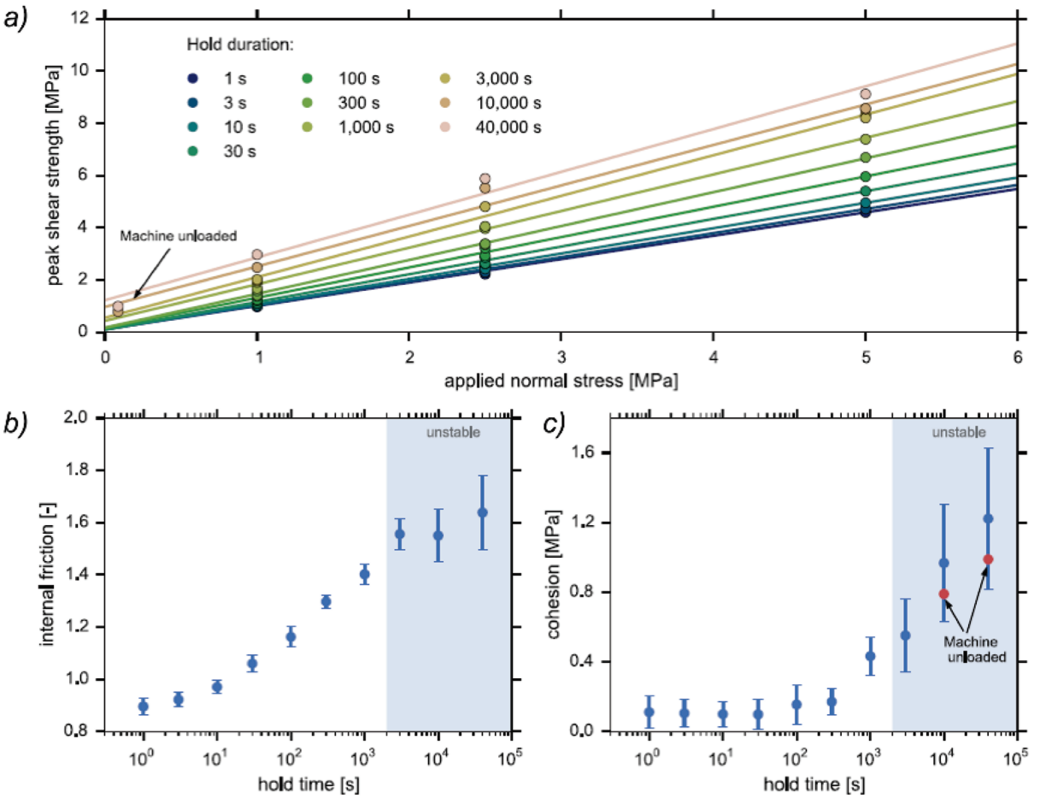

Figure 4: Data derived from slide-hold-slide experiments on brine-saturated salt gouges (from Van den Ende & Niemeijer 2019). a) Peak shear stress upon-research as a function of applied normal stress for different holds b) Values of the slopes (=internal friction) as a function of hold time c) Values of the intercepts (=cohesion) as a function of hold time.

6 Microstructures

In Figure 5, we show some representative microstructures of salt gouges sheared in the presence of saturated brine. Gouges sheared at relatively low velocity (< 10 μm/s) display low porosity domains separated by fractured domains at a low angle to the shear zone

boundary (Riedel shear, Logan et al. 1992). In contrast, gouges sheared at higher velocity show high porosities (estimated ~20-25%), in domains that are either parallel or at low angle to the shear zone boundary. Notably, a boundary parallel domain is present which is characterized by severe grain size reduction compared to the remainder of the gouge layer (boundary shear). Similar microstructures are observed for samples deformed under room-dry conditions or in the presence of a chemically inert conditions for all sliding velocities. The presence of the boundary shear seems to be correlated to the occurrence of frictionally unstable sliding.

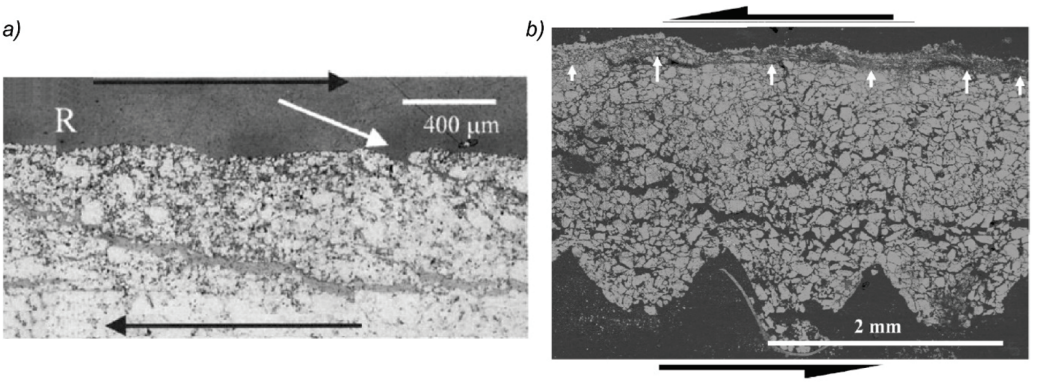

Figure 5: Examples of microstructures obtained in friction experiments on brine-saturated salt gouges. a) Reflected light image of salt gouge deformed at 2 µm/s and 1 MPa normal stress with a smooth halite wall rock (from Bos et al. 2000). White arrow indicates a Riedel shear, shear sense as indicated b) Backscatter Electron image of salt gouge deformed at 100 □m/s and 5 MPa normal stress. White arrows indicate a fine-grained boundary shear. Shear sense as indicated (from Niemeijer et al. 2010).

7 Summary, implications, and suggestions for future work

The frictional strength of salt gouges is controlled to a large extent by the volumetric behaviour of the gouge layer, i.e. at low sliding velocity in the presence of a chemically active fluid, compaction via pressure solution keeps the porosity of the gouge layer low, forcing localized fracturing of the gouge layer at a low angle to the shear zone boundary. In contrast, in gouges with a relatively lower activity of pressure solution compaction, grain size reduction produces a boundary parallel shear band which causes a weakening of the gouge layer and frictional unstable sliding.
This implies that the brittle reactivation of faults in salt can generate significant porosity and permeability, depending on the nature of the fluids present and on the loading rate. In the presence of brine, such porosity and permeability will be rapidly destroyed due to the fast compaction via pressure solution and the fine grain size produced during sliding.
For future work, it would be useful to establish how fault-parallel and fault-perpendicular permeability of brittle faults in salt evolves with slip and time and to contrast the behaviour of the simulated gouges in the presence of brine vs. that in the presence of H_2 or CO_2 and of mixtures of these.

References

BOS, B., PEACH, C. J. & SPIERS, C. J. 2000. Slip behavior of simulated gouge-bearing faults under conditions favoring pressure solution. Journal of Geophysical Research: Solid Earth, 105, 16699-16717.

BOS, B. & C. J. SPIERS, C. J. 2002. Fluid-assisted Healing Processes in Gouge-bearing Faults: Insights from Experiments on a Rock Analogue System. Pure and Applied Geophysics, 159, 2537-2566.

BUIJZE, L., NIEMEIJER, A. R., HAN, R., SHIMAMOTO, T. & SPIERS, C. J. 2017. Friction properties and deformation mechanisms of halite(-mica) gouges from low to high sliding velocities. Earth and Planetary Science Letters, 458, 107-119.

DAVISON, I. 2009. Faulting and fluid flow through salt. Journal of the Geological Society, 166, 205-216.

DIETERICH, J. H. 1979. Modeling of Rock Friction I. Experimental Results and Constitutive Equations. Journal of Geophysical Research, 84.

HEATON, T. H. 1990. Evidence for and implications of self-healing pulses of slip in earthquake rupture. Physics of the Earth and Planetary Interiors, 64, 1-20.

LOGAN, J. M., DENGO, C. A., HIGGS, N. G. & WANG, Z. Z. 1992. Fabrics of experimental fault zones - their developement and relationship to mechanical behavior. eds. B. Evans & T.-f. Wong. Elseview.

MARONE, C. 1998. Laboratory-derived friction laws and their application to seismic faulting. Annual Review of Earth and Planetary Sciences, 26, 643-696.

NIEMEIJER, A., FAGERENG, Å., IKARI, M., NIELSEN, S. & WILLINGSHOFER, E. 2020. Faulting in the laboratory. In Understanding Faults, 167-220.

NIEMEIJER, A., MARONE, C. & ELSWORTH, D. 2008 Healing of simulated fault gouges aided by pressure solution: Results from rock analogue experiments. Journal of Geophysical Research, 113.

--- 2010 Frictional strength and strain weakening in simulated fault gouge: Competition between geometrical weakening and chemical strengthening. Journal of Geophysical Research, 115.

NIEMEIJER, A. R. & SPIERS, C. J. 2006. Velocity dependence of strength and healing behaviour in simulated phyllosilicate-bearing fault gouge. Tectonophysics, 427, 231-253.

RUINA, A. 1983. Slip Instability and State Variable Friction Laws. Journal of Geophysical Research, 88.

SCHLÉDER, Z., URAI, J. L., NOLLET, S. & HILGERS, C. 2008. Solution-precipitation creep and fluid flow in halite: a case study of Zechstein (Z1) rocksalt from Neuhof salt mine (Germany). International Journal of Earth Sciences, 97, 1045-1056.

SCUDERI, M. M. & COLLETTINI, C. 2018. Fluid Injection and the Mechanics of Frictional Stability of Shale-Bearing Faults. Journal of Geophysical Research: Solid Earth, 123, 8364-8384.

SHIMAMOTO, T. 1986. Transition between frictional slip and ductile flow for halite shear zones at room temperature. Science, 231, 711-714.

VAN DEN ENDE, M. P. A. & NIEMEIJER, A. R. 2019. An investigation into the role of time-dependent cohesion in interseismic fault restrengthening. Sci Rep, 9, 9894.

ZHUO, Q.-G., MENG, F.-W., SONG, Y., YANG, H.-J., LI, Y. & NI, P. 2013. Hydrocarbon migration through salt: evidence from Kelasu tectonic zone of Kuqa foreland basin in China. Carbonates and Evaporites, 29, 291-297.